Separation Science and Technology
Publication details, including instructions for authors and subscription information:
http://www.informaworld.com/smpp/title~content=t713708471

Uranium Sorption on Solid Aluminosilicate Phases under Caustic Conditions

J. Addai-Mensah[a]; J. Li[a]; M. Zbik[a]; W. R. Wilmarth[b]
[a] Ian Wark Research Institute, University of South Australia, Mawson Lakes, Adelaide, Australia [b] Savannah River National Laboratory, Westinghouse Savannah River Company, Aiken, SC, USA

To cite this Article Addai-Mensah, J. , Li, J. , Zbik, M. and Wilmarth, W. R.(2005) 'Uranium Sorption on Solid Aluminosilicate Phases under Caustic Conditions', Separation Science and Technology, 40: 1, 267 — 279
To link to this Article: DOI: 10.1081/SS-200042003
URL: http://dx.doi.org/10.1081/SS-200042003

Separation Science and Technology, 40: 267–279, 2005
ISSN 0149-6395 print/1520-5754 online
DOI: 10.1081/SS-200042003

Uranium Sorption on Solid Aluminosilicate Phases under Caustic Conditions

J. Addai-Mensah, J. Li, and M. Zbik
Ian Wark Research Institute, University of South Australia,
Mawson Lakes, Adelaide, Australia

W. R. Wilmarth
Savannah River National Laboratory, Westinghouse Savannah
River Company, Aiken, SC, USA

Abstract: The formation of aluminosilicate scales in the High Level Waste Evaporators at the Savannah River Site led to curtailed operation and an expensive cleaning evolution due in part to the presence of enriched uranium in the scale. Therefore, the sorption behavior of uranium species and sodium aluminosilicate (NAS) solid phases in nitrate/nitrite-rich sodium aluminosilicate solutions were studied under well-defined conditions at 22°C and agitation rate of 400 rpm. The NAS solids comprised four well-characterized phases of amorphous, zeolite A, sodalite, and cancrinite. Pure, synthetic sodium diuranate ($Na_2U_2O_7$) crystals were precipitated and used as the base/reference U-containing compound.

The studies of the sorption behavior of U-containing species on NAS solid phases were conducted under conditions where no detectable dissolution, precipitation, or crystallographic phase transformation of the NAS adsorbent phases were observed over a 6 h test period. The uranium sorption capacities were reached typically within 3 h. The uranium capacities were measured 6.36 to 9.3 mg U kg^{-1} NAS solid for the Zeolite A and cancrinite phase. The amorphous and sodalite phase had higher uranium loading that measured between 19 and 58 mg U kg^{-1} NAS solid.

Address correspondence to J. Addai-Mensah, Ian Wark Research Institute, University of South Australia, Mawson Lakes, Adelaide 5095, Australia. E-mail: Bill.Wilmarth@SRS.gov

INTRODUCTION

Effective management of High Level Waste (HLW) products during hydrothermal processing in waste evaporators is crucial to the Savannah River Site (SRS) tank farm operations. The formation and accumulation of waste products comprising sodium aluminosilicate (NAS) solid polytypes (e.g., amorphous, zeolite, sodalite, and cancrinite) and uranium-based solids (e.g., sodium diuranate) that are enriched in fissionable uranium lead to a serious fouling problem and criticality concern (1, 2). The control, handling, and mitigation of this serious fouling issue pose a major technological challenge, warranting systematic studies that will provide a greater understanding and new knowledge of the mechanism of fouling, particularly uranium incorporation into NAS phases (3–5).

Several parallel processes are involved in the formation of various sodium aluminosilicate phases and uranium-based solids. Examples are transport, sorption desorption, and incorporation of solution reactant species, particle–particle interactions and growth, etc. The mechanisms involved in NAS precipitation and incorporation of uranium species may be substantially influenced by crystallochemical structure of NAS phases present. Our understanding of the fundamental mechanisms underpinning NAS precipitation under conditions typical of those prevailing in HLW evaporators is now better understood (2).

To date, there exist a number of unresolved issues regarding the sodium aluminosilicate fouling and uranium incorporation processes. Mechanistic information gleaned from recent SRNL crystallization and characterization studies (6, 7) are inconclusive. Of particular interest are the mechanisms by which the uranium-based particles are formed or how the uranium-containing species or growth units may sorb or be accommodated crystallographically with or within the sodium aluminosilicate solid matrix. Therefore, the investigation examines the most basic interaction: sorption of uranium onto the aluminosilicate phases to determine its contribution to the uranium loading in the NAS scale.

EXPERIMENTAL

Sorption, as used in this report, is defined as an interfacial process where U-containing species in solution bind in the inner electrical double layer on NAS solid phase, leading to a significant decrease in bulk solution concentration. The exact nature of the U-containing species involved in sorption is not known, but it may comprise monomeric, and/or polymeric, oxo- and/or hydroxobridged ionic complexes. Sorption experiments were conducted by seeding the test solutions with known masses and surface areas of the NAS solid phase and the suspensions agitated at 400 rpm under well-sealed conditions. The composition of the waste simulant was 4 M NaOH, 1 M $NaNO_3$, and 1 M $NaNO_2$. The amount of silicon and aluminum contained in the simulant was determined by the NAS phase solubility. Slurry samples were taken periodically for U, Al(III), and SiO_2 analysis over 6 h. The samples were then centrifuged at 15,000 rpm for 20 min and the supernatant filtered through an 0.1 μm Teflon membrane for solution concentration analysis.

To obtain detectable sorption behavior, two extremely high levels of total particle surface area 12,240 and 24,480 $m^2\,dm^{-3}$, corresponding to massive NAS seed mass charge, typically in the range 160–1102 $g\,dm^{-3}$ were used. It is noted that a very high NAS seed charge (e.g., ~1 $kg\,dm^{-3}$ liquor) was required for the low specific surface area zeolite A material used in these tests in order to produce a detectable U sorption loading. On the other hand, a lower solid loading of 0.16 kg solid dm^{-3} liquor was needed for a high specific surface area NAS seed material (e.g., sodalite), while ~0.33 kg solid dm^{-3} liquor was required for a phase with a moderate specific surface area (amorphous and cancrinite).

It is worth mentioning the significance of the good agitation/mixing used during U sorption onto colloidal NAS particles and the strong mixing and pulp compression achieved by centrifugation during solid-liquor separation after sorption. In an agitated solid–liquid system of high solid loading, such as the present case, species volume diffusion limitation, if it exists, is overcome with the agitation energy dissipation rate (based on power input) being high enough. The agitation rate of 400 rpm used was found to produce insignificant concentration gradient in bulk solution. Thus, solution mixing and species transport should proceed in a manner that would lead to similar species concentration in the bulk free solution and the pockets of bulk solution retained within aggregated particles. For solution trapped incages, channels, pores, and cavities of primary particles, one may expect equilibration with the bulk solution under the strong centrifugation (15,000 rpm) used in the present work to be complete at the end of sorption. Consequently, representative solutions should emerge for U, Al(III), and SiO_2 concentrations. The concentration difference-centrifugation approach employed in the present work is extensively used in the literature (8) as a standard, indirect method for quantification of sorption loading.

Prior to initiating the sorption experiments and to exclude uranium precipitation due to uranium supersaturation, the uranium equilibrium solubility of sodium diuranate was measured over 30 days at 22°C. Figure 1 shows a typical approach to equilibrium from "above" and "below" during solubility determination by both precipitation and dissolution. It is observed that a good agreement was obtained between approaches. The uranium concentration was observed to reach its equilibrium value within 10 days and remained substantially constant over 30 days. No significant change in SiO_2 and Al(III) concentrations was observed over the period.

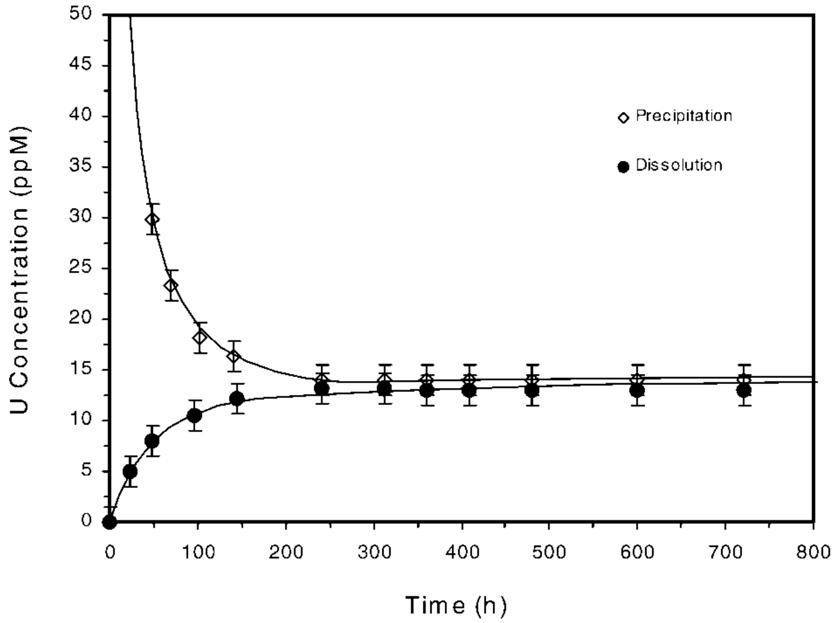

Figure 1. Variation of U concentration with time during both dissolution and precipitation of sodium diuranate in 4.0 M NaOH, $NaNO_3 = 1.0$ M, $NaNO_2 = 1.0$ M, $SiO_2 = 1.7 \times 10^{-3}$ M, and Al(III) = 17.0×10^{-3} M solutions at 22°C (precipitation: U = 3400 ppm; seed charge of $Na_2U_2O_7 = 50\,g\,dm^{-3}$).

The results show that under solution conditions described in Table 1, uranium solubility in liquors containing $NaOH = 4.0$ M, $NaNO_3 = 1.0$ M, $NaNO_2 = 1.0$ M, $SiO_2 = 0.5 \times 10^{-3} - 75.0 \times 10^{-3}$ M, and $(6.6 - 133.5) \times 10^{-3}$ M Al(III) were in the range 13.4 to 15.3 ± 0.5 ppm uranium. The observed solubility trends are in agreement with reported studies (9–12). Consequently, all the sorption studies with liquor composition within this range were performed at constant solution uranium concentration of 15.0 ± 0.5 ppm. During testing, the silicon and aluminum concentrations were measured by Inductively Coupled Plasma—Emission Spectroscopy, and the uranium was measured by Inductively Coupled Plasma—Mass Spectrometry.

RESULTS AND DISCUSSION

Figures 2–5 show uranium sorption onto the different NAS seed phases as a function of time. The sorption loading increased with time and eventually reached a plateau value corresponding to an “equilibrium” U concentration in solutions after 3 h. The measurements for each NAS solid phase were

Table 1. Uranium equilibrium solubility of sodium diuranate ($Na_2U_2O_7$) crystals in nitrated/nitrited caustic aluminosilicate liquors measured at 22°C

	Initial solution composition					
Related NAS phase	NaOH (M)	$NaNO_3$ (M)	$NaNO_2$ (M)	SiO_2 ($\times 10^{-3}$ M)	Al(III) ($\times 10^{-3}$ M)	Solubility U (ppm or mg dm^{-3})
Amorphous	4.0	1.0	1.0	45.0	133.4	15.3 ± 0.5
	4.0	1.0	1.0	59.6	120.0	15.2 ± 0.5
	4.0	1.0	1.0	55.0	125.0	15.0 ± 0.5
	4.0	1.0	1.0	74.0	100.0	14.9 ± 0.5
Zeolite	4.0	1.0	1.0	4.5	100.7	15.1 ± 0.5
	4.0	1.0	1.0	10.0	65.0	14.4 ± 0.5
	4.0	1.0	1.0	12.3	48.2	14.2 ± 0.5
	4.0	1.0	1.0	14.5	32.0	13.8 ± 0.5
Sodalite	4.0	1.0	1.0	2.6	85.6	15.2 ± 0.5
	4.0	1.0	1.0	5.0	40.0	14.2 ± 0.5
	4.0	1.0	1.0	9.6	20.3	13.5 ± 0.5
	4.0	1.0	1.0	12.1	16.2	13.4 ± 0.5
Cancrinite	4.0	1.0	1.0	0.5	85.6	15.1 ± 0.5
	4.0	1.0	1.0	1.7	17.0	13.6 ± 0.5
	4.0	1.0	1.0	1.8	13.0	13.5 ± 0.5
	4.0	1.0	1.0	2.5	6.6	13.4 ± 0.5

replicated three times for a given solution composition. Hence, the reported values are the arithmetic means. As shown in Table 2, the initial uranium concentration of 15.0 ppm decreased by 20–50% upon sorption, depending upon the NAS phase used and Al(III)/SiO_2 concentration.

From the surface area-weighted U sorption loadings in Figs. 2–5, it appeared that the higher loading resulted from lower seed charge (12,240 m^2 dm^{-3}) as compared with a higher seed charge (24,480 m^2 dm^{-3}). This feature, however, may be largely attributed to a surface area effect, as the doubling in NAS seed particle surface area did not reflect in a corresponding increase in amount of U sorbed or concomitant decrease in solution U species, except for the particular case of cancrinite seeding (Fig. 5). Only a subtle decrease in solution U concentration occurred when the surface area was doubled. The NAS particle surface area effect suggests that the availability of a certain number of favorable NAS phase-specific sorption sites per total surface plays a crucial role in U sorption loading. The remarkably low U loading behavior is perceived to be due to the nature of speciation and the fact that only a limited fraction of the total U species in solution may be thermodynamically predisposed to undergo sorption.

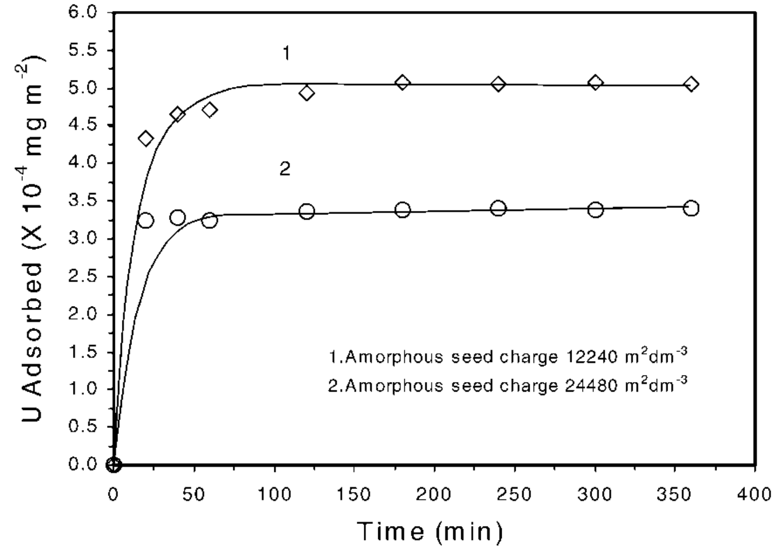

Figure 2. Sorption of uranium onto amorphous seed surface as a function of time at 22°C (solution concentration: NaOH = 4.0 M, $NaNO_3$ = 1.0 M, $NaNO_2$ = 1.0 M, $SiO_2 = 1.7 \times 10^{-3}$ M, Al(III) = 2.7×10^{-3} M, and U = 15.0 ppm).

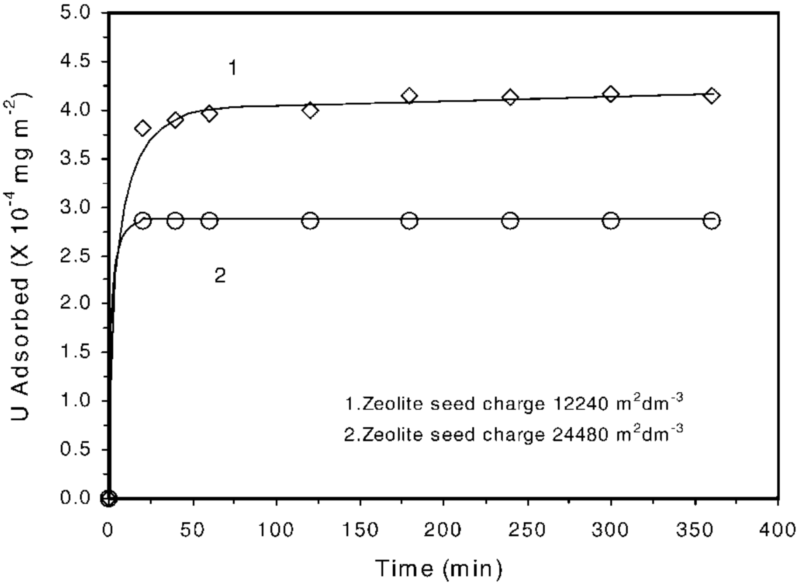

Figure 3. Sorption of uranium on zeolite seed particles as a function of time at 22°C (solution concentration: NaOH = 4.0 M, $NaNO_3$ = 1.0 M, $NaNO_2$ = 1.0 M, $SiO_2 = 1.7 \times 10^{-3}$ M, Al(III) = 2.7×10^{-3} M, and U = 15.0 ppm).

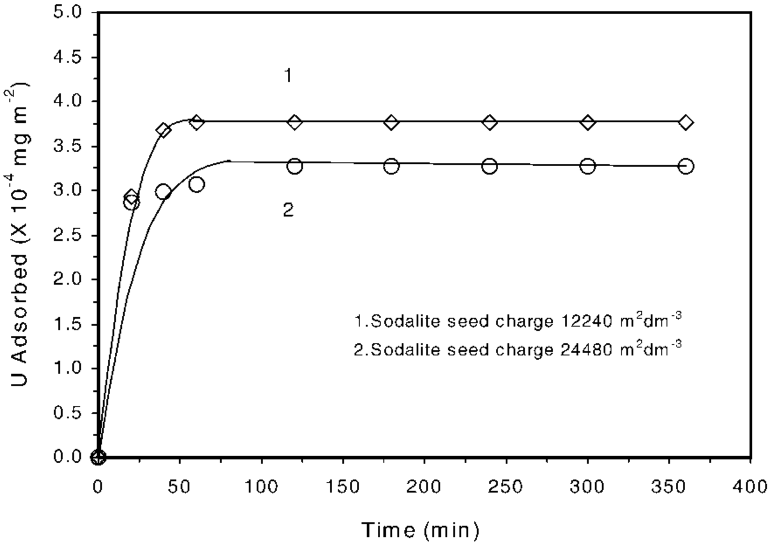

Figure 4. Sorption of uranium onto sodalite seed particles as a function of time at 22°C (solution concentration: $NaOH = 4.0\,M$, $NaNO_3 = 1.0\,M$, $NaNO_2 = 1.0\,M$, and $U = 15.0\,ppm$).

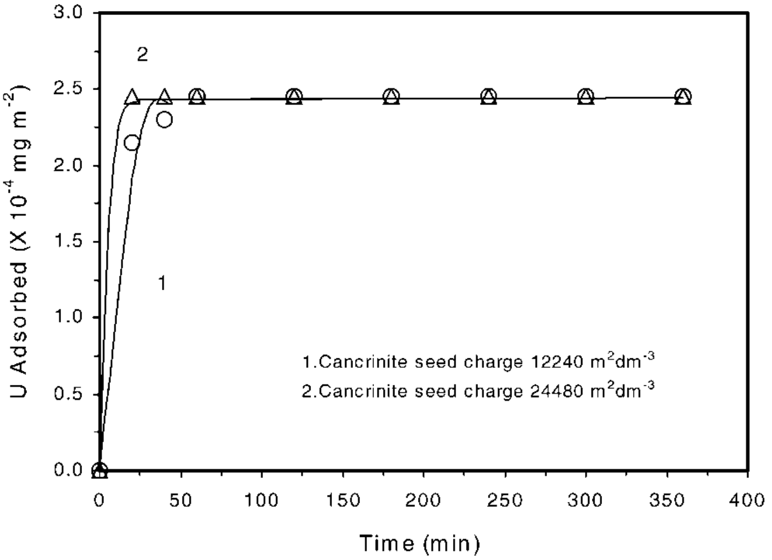

Figure 5. Sorption of uranium on cancrinite seed particle as a function of time at 22°C (initial solution concentration: $NaOH = 4.0\,M$, $NaNO_3 = 1.0\,M$, $NaNO_2 = 1.0\,M$, and $U = 15.0\,ppm$).

Table 2. Uranium (VI), SiO_2, and Al(III) concentrations in solutions after 6 h sorption tests at 22°C (solution concentration: NaOH = 4.0 M, $NaNO_3$ = 1.0 M, $NaNO_2$ = 1.0 M, and U = 15.00 ppm)

	Seed charge		U sorption loading	Final concentration		
Seed	($m^2\,dm^{-3}$)	($kg\,dm^{-3}$)	U/SAS ($mg\,kg^{-1}$)	U(VI) (ppm or $mg\,dm^{-3}$)	SiO_2 ($\times 10^{-3}$ M)	Al(III) ($\times 10^{-3}$ M)
Amorphous	12,240	0.17	36.47	8.8 ± 0.3	72.9 ± 1.8	98.2 ± 2.5
	24,480	0.34	24.41	6.7 ± 0.2	59.6 ± 1.5	122.0 ± 3.1
	12,240	0.17	32.35	9.5 ± 0.3	65.1 ± 1.6	110.5 ± 2.8
	12,240	0.17	23.52	11.0 ± 0.4	41.9 ± 1.1	133.4 ± 3.3
Zeolite	12,240	0.55	9.27	9.9 ± 0.4	14.0 ± 0.4	31.6 ± 0.8
	24,480	1.10	6.36	8.0 ± 0.3	11.2 ± 0.3	50.4 ± 1.3
	12,240	0.55	8.00	10.6 ± 0.4	13.2 ± 0.3	45.0 ± 1.1
	12,240	0.55	6.55	11.4 ± 0.4	4.6 ± 0.2	100.7 ± 2.5
Sodalite	12,240	0.08	57.5	10.4 ± 0.4	12.4 ± 0.3	15.8 ± 0.4
	24,480	0.16	50.0	7.0 ± 0.3	11.9 ± 0.3	16.9 ± 0.4
	12,240	0.08	48.75	11.1 ± 0.4	9.8 ± 0.2	19.6 ± 0.5
	12,240	0.08	18.75	12.0 ± 0.4	2.6 ± 0.1	85.6 ± 2.1
Cancrinite	12,240	0.33	9.09	12.0 ± 0.4	2.5 ± 0.1	6.6 ± 0.2
	24,480	0.66	8.69	9.0 ± 0.3	2.3 ± 0.1	6.7 ± 0.2
	12,240	0.33	7.58	12.5 ± 0.5	1.8 ± 0.1	13.0 ± 0.3
	12,240	0.33	9.09	12.0± 0.4	0.5 ± 0.02	89.0 ± 2.2

Under the conditions used in the investigations, enhanced interactions with the amorphous material, zeolite A, and sodalite particle surfaces was not facilitated by the presence of a much higher surface area loading. Once a sufficient number of sites for sorption are available and they accommodate all the "sorbable" uranium species, a dynamic equilibrium appears to be established, within 3 h, with the remaining nonsorbing U species in solution. Hence, no further sorption occurred, even though excess particle surface sites existed. In other words, the remaining U species in solution were practically nonadsorbing.

The NAS phase had a marked impact on the U loading as indicated by the range of final U concentrations measured in solution at the end of the experiment as shown below.

Amorphous seeds: 6.7–11.0 ppm

Zeolite A crystals: 8.0–11.4 ppm

Sodalite crystals: 7.0–12.4 ppm

Cancrinite crystals: 9.0–12.5 ppm

Taking cognizance of the analytical limit of U detection being 1 ppb by the ICP/MS technique used and the experimental pure error of 0.5 ppm, the differences are significant. The observed U loading indicates a low affinity type of sorption behavior for all the four NAS solid phases. The variations in the equilibrium U value for each NAS adsorbent phase and between the phases may be rationalized in terms of the specific NAS crystallochemical characteristics and related Al(III) and SiO_2 concentrations and, perhaps, the influence of solution speciation (13).

Figures 6 and 7 show a strong NAS phase-dependent U sorption loading behavior for a given Al(III) concentration. The following U loading sequence was established on an equivalent NAS solid surface area basis:

$$\text{Amorphous} > \text{Zeolite A} > \text{Sodalite} > \text{Cancrinite}$$

On the basis of the present sorption data, it may be concluded that amorphous NAS is the most effective sorbent for the removal of U species from HLW type of solutions. The greater effectiveness of the amorphous phase as a sorbent is consistent with the studies of Ball et al. (14), which reported amorphous $Ti(OH)_4$ as a most efficient sorbent for hydrated uranyl species.

In terms of solid mass loading, a different U sorption loading trend emerged, as indicated below and also detailed in Table 2:

Amorphous: 23.5–36.5 mg U kg^{-1} NAS solid.

Zeolite A: 6.6–9.3 mg U kg^{-1} NAS solid.

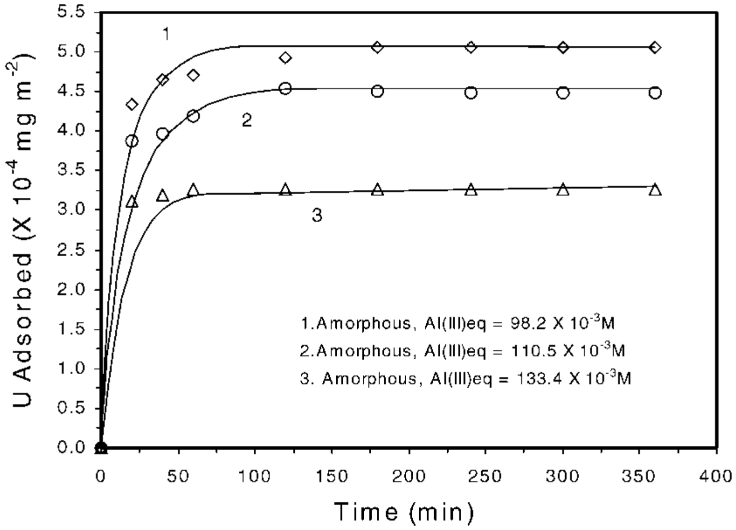

Figure 6. Sorption of uranium onto amorphous seed surface as a function of time and different Al(III) concentration at constant seed charge and 22°C (solution concentration: NaOH = 4.0 M, $NaNO_3$ = 1.0 M, $NaNO_2$ = 1.0 M, and U = 15.0 ppm; seed charge = 12,240 m^2 dm^{-3}).

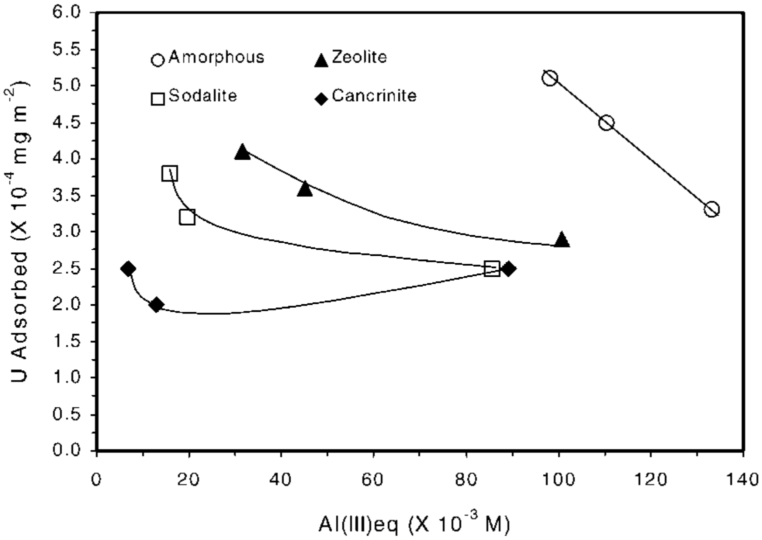

Figure 7. Variation of sorption loading of uranium on different seed surface as a function of Al(III) concentration (solution concentration: NaOH = 4.0 M, $NaNO_3$ = 1.0 M, $NaNO_2$ = 1.0 M, SiO_2 = 1.7–75.0 × 10^{-3} M, and U = 15.0 ppm; seed charge = 12,240 m^2 dm^{-3}).

Sodalite: 18.8–57.5 mg kg^{-1} NAS solid.

Cancrinite: 7.6–9.1 mg kg^{-1} NAS solid.

When a basis of an equivalent solid mass loading (1 kg per dm^3) and at a given Al(III) concentration is used, the sorption loading decreased in the following manner:

$$\text{Sodalite} > \text{Amorphous} > \text{Cancrinite} \geq \text{Zeolite A}$$

Further analysis of the results revealed that the equilibrium Al(III) concentration in solution played a key role in the U sorption behavior (Fig. 6). The results indicated that the sorption loading decreased markedly with increasing Al(III) equilibrium concentration for all four types of NAS seeds (Fig. 7). To confirm the influence of Al(III) concentrations on sorption behavior, further tests were performed as a function of initial Al(III) concentrations at a constant cancrinite seed charge of 12,240 $m^2\,dm^{-3}$. The data plotted in Fig. 8 demonstrate that increasing the Al(III) concentration to 133.4×10^{-3} M resulted in a significant decrease in U sorption loading. The dependency of U sorption behavior on sorbent type and its characteristics are consistent with reported studies of radionuclides uptake onto zeolitic and

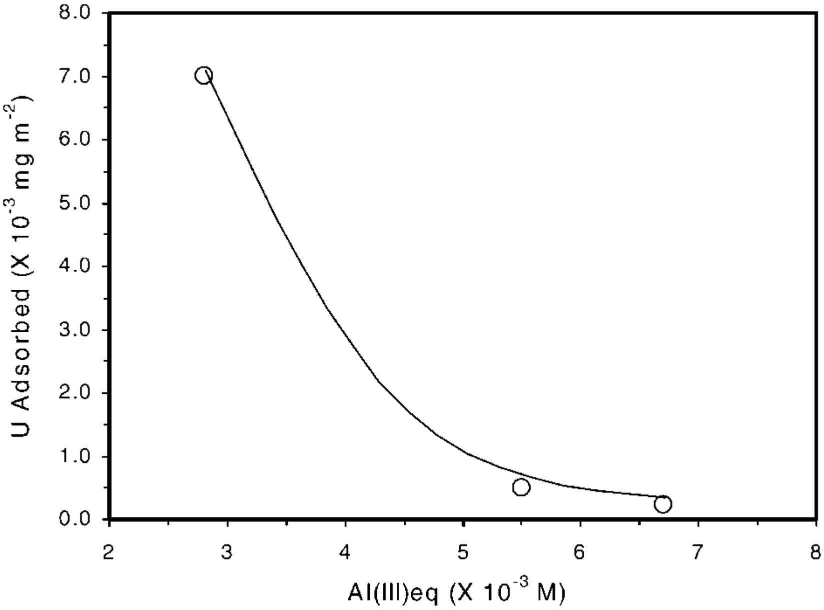

Figure 8. Variation of uranium sorption loading onto cancrinite seed surface as a function of Al(III) concentration.

alumina solid phases (15) or titanosilicates, layered manganese oxides and antimonysilicate solids (16).

CONCLUSIONS

The sorption studies carried out under well-defined conditions where no noticeable dissolution, precipitation, and crystallographic phase transformation of the NAS adsorbent phases occurred over 6 h showed a clear trend of Al(III) concentration dependent and NAS solid phase specific U sorption behavior. The U sorption loading decreased with increasing Al(III) concentration and with the thermodynamic stability of the NAS phase used at equivalent surface area of NAS sorbent. The observed sorption behavior is a low affinity when compared with the results of other studies involving zeolitic and alumina solid phases (15).

REFERENCES

1. Wilmarth, W.R., Thompson, M.C., Martino, C.J., Dukes, V.H., Mills, J.T., Boley, C., and Lewis, B.L. (2003) Nitric Acid Cleaning of a Sodalite–Sodium Diuranate Scale in High Level Waste Evaporators. *Sep. Sci. Technol.*, 38 (12&13): 3249–3271.
2. Wilmarth, W.R., Rosencrance, S.W., Hobbs, D.T., Jantzen, C.M., Laurinat, J.E., Van Pelt, W.B., Tamosaitis, W.L., Mattus, A.J., Hu, M.Z., DePaoli, D.W., Weber, C.F., McGinnis, C.P., and Mattigod, S. Aluminosilicate Formation in High Level Waste Evaporators: A Mechanism for Uranium Accumulation. *Proceedings of Waste Management '02*.
3. Gasteiger, H.A., Frederick, W.J., and Streisel, R.C. (1992) Solubility of Aluminosilicates in Alkaline Solutions and a Thermodynamic Equilibrium Model. *Ind. Eng. Chem. Res.*, 31: 1183–1190.
4. Barnes, M.C., Addai-Mensah, J., and Gerson, A.R. (1999) The Solubility of Sodalite and Cancrinite in Synthetic Spent Liquor. *Colloids Surf. A*, 157 (1): 101–116.
5. Zheng, K., Addai-Mensah, J., Smart, R.St.C., and Gerson, A.R. (1998) Solubility of Sodium Aluminosilicates in Synthetic Bayer Liquor. *J. Chem. Eng. Data.*, 43 (3): 312–317.
6. Oji, L. and Williams, A. (2002) WSRC Report No. SRT-LWP-2002-00109.
7. Duff, M. (2002) WSRC Report No. SRT-LWP-2002-00109.
8. Fleer, G.J., Cohen, M.A., Stuart, J.M., Scheutjens, H.M., and Cosgrove, Vincent T.B. (1993) *Polymer at Interfaces*; Chapman and Hall: London.
9. Peterson, R.A. and Pierce, R.A. *Sodium Diuranate and Sodium Aluminosilicate Precipitation Testing Results*, WSRC-TR-2000-00156, May 15, 2000.
10. Hobbs, D.T. and Edwards, T.B. *Solubility of Uranium in Alkaline Salt Solutions (U)*, WSRC-TR-93-454, March 29, 1994.

11. Puigdomenech, I. and Bruno, J. (1988) *Modeling Uranium Solubilities in Aqueous Solutions: Validation of a Thermodynamic Database for the EQ 3/6 Geochemical Codes*, Swed. SKB Tech. Rep., SKB 88-21.
12. Cordfunke, E.G.P. and Loopstra, B.O. (1971) Sodium Uranates; Preparation and Thermochemical Properties. *J. Inorg. Nucl. Chem.*, 33: 2427–2436.
13. Clark, D.L. and Fedosseev, A.M. Actinide-Aluminate Speciation in Alkaline Radioactive Waste, Final Report, U.S. Department of Energy, September 9, 2001.
14. Ball, C.J., Buykx, W.J., Dickson, F.J., Hawkins, K., Levins, D.M., Smart, R.St.C., Smith, K.L., Stevens, G.T., Watson, K.G., Weedon, D., and White, T. (1989) Titanate Ceramics for the Stabilization of Partially Reprocessed Nuclear Fuel Elements. *J. Am. Ceram. Soc.*, 72 (3): 404–414.
15. Azenha, M.E.D.G., da Graca Miguel, M., Formosinho, S.J., and Burrows, H.D. (2001) The Characterisation by Luminescence Spectroscopy of Uranium(VI) Incorporated into Zeolites and Aluminas. *J. Mol. Struct.*, 563–546: 439–442.
16. Al-Attar, L., Dyer, A., and Harjula, R. (2003) Uptake of Radionuclides on Macroporous and Layered Ion Exchange Materials. *J. Mater. Chem.*, 13: 2963–2968.